SCIENCE CHINA
Technological Sciences

Progress of Projects Supported by NSFC

September 2013 Vol.56 No.9: 2268–2277
doi: 10.1007/s11431-013-5303-5

Correction method for non-landing measuring of vehicle-mounted theodolite based on static datum conversion

LIU JinBo[1,2], ZHANG XiaoHu[1,2*], LIU HaiBo[1,2], YUAN Yun[1,2], ZHU ZhaoKun[1,2] & YU QiFeng[1,2]

[1] *College of Aerospace Science and Engineering, National University of Defense Technology, Changsha 410073, China;*
[2] *Hunan Key Laboratory of Videometrics and Vision Navigation, Changsha 410073, China*

Received April 17, 2013; accepted July 3, 2013; published online July 29, 2013

During the non-landing measuring of vehicle mounted theodolite, especially under high-speed tracking measurement, the misalignment of theodolite's center of mass and spindle etc. will cause high-frequency vibration of theodolite platform, increase the observation error of targets and even unbelievable results. In this paper, a correction method of non-landing measuring of theodolite based on static datum conversion is presented, which can effectively improve the observation accuracy of theodolite. The CCD camera is fixed to the theodolite platform to calculate the gesture shaking quantity of theodolite platform in geodetic coordinate system through the real time imaging of static datum. The observation results of theodolite are corrected by using such shaking quantity. The experiment shows that the correction accuracy exceeds 10 s of arc. The intrinsic parameter calibration technology of camera based on stellar angular distance and absolute conic put forward in this paper can prevent the estimated error of extrinsic parameters influencing the intrinsic parameter calibration and improve the intrinsic parameter calibration accuracy; the static datum conversion technology can reduce the influence of installation error of camera and theodolite platform on gesture measuring of the platform. The simulation experiment shows that when the shaking range of the platform is less than 30 min of arc, the influence of the three-axis installation error of camera within 3deg on the accuracy of correction results is less than 8 s of arc. The method in this paper can be extended to and used in the field of gesture shaking measuring and micro-structure deformation of various unstable platforms, therefore it is of important theoretical research significance and has wide engineering application prospect.

vehicle-mounted theodolite, non-landing Measuring, error correction, static datum conversion, decoupling calibration

Citation: Liu J B, Zhang X H, Liu H B, et al. Correction method for non-landing measuring of vehicle-mounted theodolite based on static datum conversion. Sci China Tech Sci, 2013, 56: 2268–2277, doi: 10.1007/s11431-013-5303-5

The theodolite is the most basic tracking measuring equipment to obtain the trajectory data and flight status of flying targets and is mainly divided into the fixed-type theodolite and vehicle-mounted theodolite by work modes [1–3]. Although the fixed-type theodolite is of high accuracy and reliability, it has limited range of action and is hard to meet the maneuverable demand of modern weapons. The vehicle-mounted theodolite makes up the weakness of the fixed-type theodolite in the aspect of maneuverability by using maneuverable station distribution and fixed point measuring, that is to say, transporting the theodolite to the measuring point location by vehicle first and then carrying out measurement; in which, after arriving at the point location, the circumstance placing the theodolite on the foundation and then carrying out measurement is called "landing measuring" and the circumstance not placing the theodolite on the foundation and then carrying out measurement directly is called "non-landing measuring" [4]. However, there are some

*Corresponding author (email: zxh1302@hotmail.com)

problems in the actual use of the vehicle-mounted theodolite, for example, the landing measuring needs long preparation time, not satisfying the real-time requirements; although the non-landing measuring can effectively ensure the flexibility of the optical measurement of shooting range and extend the measuring area, it is of no fixed base, so under the working condition of theodolite, especially under high-speed tracking measurement, the theodolite's center of mass and spindle are easy to be misaligned and the eccentric torque generated hereof will make the theodolite platform shake, causing non-uniform datum coordinate system and unbelievable angle measuring results of theodolite. To extend the application of the vehicle-mounted theodolite under such conditions, the conversion relation of theodolite platform and geodetic datum at any time is calculated with high accuracy and the angle measuring results of theodolite is corrected, then the measuring results under geodetic datum coordinate system will be obtained.

Ref. [5] demonstrates by numerical simulation experiment that the rotational deformation is the main factors to influence the angle measuring error of theodolite. The relation model of angle measuring error of the vehicle-mounted theodolite and rotational deformation angle is established. The deviation angle of the platform is measured by using the Moire fringe auto-collimation measuring system and the slope angle of the platform is measured by using inclinometer to correct the measuring results of theodolite; in ref. [6], the shaking quantity of the vehicle-mounted platform is imaged on the CCD target surface in the auto-collimation collimator by light path transmission, the video signal is collected by image capture card from time to time and the gesture shaking quantity of the platform is calculated based on the interpreted miss distance quantity data; a relative measuring method to calculate the three-dimensional motion of unstable platform is put forward in ref. [7], however, in the actual outdoor working environment, the initial gesture of theodolite and alignment accuracy of geodetic coordinate system are hard to be ensured.

A non-contact absolute measuring method based on camera measurement is put forward in this paper and the gesture rotation matrix is calculated by the real-time imaging of static datum with CCD camera [8, 9]. As the pointing of static datum in inertial space is not changed, the angle measuring results of the vehicle-mounted theodolite at any time can be corrected to the geodetic coordinate system.

1 Mathematical analysis

1.1 Definition of coordinate system

To elaborate the correction measuring principles in this paper, some common right-handed coordinate systems of theodolite are introduced.

Platform coordinate system of theodolite: The origin is the intersection point of the horizontal axis and vertical axis of theodolite, *Y* axis coincides with the vertical axis of theodolite, *Z* axis coincides with the vertical axis at initial moment, *X* axis is confirmed by the right-handed rule and the coordinate system is fixed to and moves with the theodolite platform; the horizontal axis of theodolite and the geodetic horizontal plane at initial moment are parallel and point to the north. The vertical axis points to the earth's core and is in vertical state.

Geodetic coordinate system: It coincides with the platform coordinate system of theodolite at initial moment and is not changed in inertial space.

Camera coordinate system: The origin is the optical center of camera and the *Z* axis coincides with the optical axis of camera and moves with the camera.

Image coordinate system: The origin is at the top left corner of the image and it is a rectangular coordinate system with pixel as the coordinate unit.

Inertial coordinate system: The origin is the earth's center, the *X* axis points to the intersection point of equatorial plane and prime meridian, the *Z* axis coincides with the earth axis and the *Y* axis is confirmed by the right-handed rule.

The static datum coordinate system is established on marker and keeps relatively static with the geodetic coordinate system.

1.2 Absolute conic

The absolute conic $\boldsymbol{\Omega}_\infty$ is a conic on infinite plane π_∞. In the measuring coordinate system, $\pi_\infty=(0, 0, 0, 1)$ and the point $\boldsymbol{X}=(x_1, x_2, x_3, x_4)^{\mathrm{T}}$ in $\boldsymbol{\Omega}_\infty$ satisfies

$$\left.\begin{aligned} x_1^2+x_2^2+x_3^2=0,\\ x_4^2=0. \end{aligned}\right\} \tag{1}$$

The equation of $\boldsymbol{\Omega}_\infty$ can be written as

$$\left(x_1\ x_2\ x_3\right)\boldsymbol{I}_{3\times3}\left(x_1\ x_2\ x_3\right)^{\mathrm{T}}=0. \tag{2}$$

It is clear that it is a conic comprising pure imaginary points on π_∞.

Once the $\boldsymbol{\Omega}_\infty$ is identified in the three-dimensional projective space, the included angle in the Euclidean coordinate system can also be measured. Assuming that the direction vectors of two straight lines are $\boldsymbol{d}_1$ and $\boldsymbol{d}_2$ respectively (generally not unit vectors), its included angle in the Euclidean coordinate system is

$$\cos\theta=\frac{\boldsymbol{d}_1^{\mathrm{T}}\boldsymbol{d}_2}{\sqrt{\left(\boldsymbol{d}_1^{\mathrm{T}}\boldsymbol{d}_1\right)\left(\boldsymbol{d}_2^{\mathrm{T}}\boldsymbol{d}_2\right)}}. \tag{3}$$

Or it can be written as

$$\cos\theta=\frac{\boldsymbol{d}_1^{\mathrm{T}}\boldsymbol{\Omega}_\infty\boldsymbol{d}_2}{\sqrt{\left(\boldsymbol{d}_1^{\mathrm{T}}\boldsymbol{\Omega}_\infty\boldsymbol{d}_1\right)\left(\boldsymbol{d}_2^{\mathrm{T}}\boldsymbol{\Omega}_\infty\boldsymbol{d}_2\right)}}. \tag{4}$$

1.3 Absolute conic and intrinsic parameter matrix

The point on π_∞ can be written as $\boldsymbol{X}_\infty=(\boldsymbol{d}^{\mathrm{T}}, 0)^{\mathrm{T}}$, and is imaged as image point x by general camera

$$x=\boldsymbol{P}\boldsymbol{X}_\infty=\boldsymbol{K}\boldsymbol{R}\left[\boldsymbol{I}\mid -\boldsymbol{C}\right]\begin{pmatrix}\boldsymbol{d}\\0\end{pmatrix}=\boldsymbol{K}\boldsymbol{R}\boldsymbol{d}=\boldsymbol{H}\boldsymbol{d}. \tag{5}$$

The $\boldsymbol{H}$ is the planar homography matrix, that is to say, mapping between infinite plane and image plane.

Under point transformation $x=\boldsymbol{H}\boldsymbol{d}$, the deduction of conic conversion is as follows:

$$\begin{aligned}\boldsymbol{d}^{\mathrm{T}}\boldsymbol{\Omega}_\infty\boldsymbol{d}&=\left(\boldsymbol{H}^{-1}x\right)^{\mathrm{T}}\boldsymbol{\Omega}_\infty\left(\boldsymbol{H}^{-1}x\right)\\&=x^{\mathrm{T}}\left(\boldsymbol{H}^{-\mathrm{T}}\boldsymbol{\Omega}_\infty\boldsymbol{H}^{-1}\right)x\\&=x^{\mathrm{T}}\boldsymbol{\Omega}'_\infty x.\end{aligned}$$

$\boldsymbol{H}=\boldsymbol{K}\boldsymbol{R}$ is substituted into the above formula:

$$\begin{aligned}\boldsymbol{\Omega}'_\infty&=(\boldsymbol{K}\boldsymbol{R})^{-\mathrm{T}}\boldsymbol{\Omega}_\infty(\boldsymbol{K}\boldsymbol{R})^{-1}\\&=\boldsymbol{K}^{-\mathrm{T}}(\boldsymbol{R}^{-\mathrm{T}}\boldsymbol{I}\boldsymbol{R}^{-1})\boldsymbol{K}^{-1}\\&=(\boldsymbol{K}\boldsymbol{K}^{\mathrm{T}})^{-1}.\end{aligned} \tag{6}$$

$\boldsymbol{\Omega}'_\infty$ is also called image of Ω_∞ which is only related to the intrinsic parameter $\boldsymbol{K}$ of camera and not related to the gesture and location of camera.

1.4 Relation of absolute conic and ray included angles

It can be seen from Figure 1 that the back projections of image points x_1 and x_2 are two rays, whose direction vectors are $\boldsymbol{d}_1$ and $\boldsymbol{d}_2$ respectively and the included angle is θ.

According to eq. (4),

$$\begin{aligned}\cos\theta&=\frac{\boldsymbol{d}_1^{\mathrm{T}}\boldsymbol{d}_2}{\sqrt{\left(\boldsymbol{d}_1^{\mathrm{T}}\boldsymbol{d}_1\right)\left(\boldsymbol{d}_2^{\mathrm{T}}\boldsymbol{d}_2\right)}}\\&=\frac{\left(\boldsymbol{K}^{-1}x_1\right)^{\mathrm{T}}\left(\boldsymbol{K}^{-1}x_2\right)}{\sqrt{\left(\boldsymbol{K}^{-1}\boldsymbol{x}_1\right)^{\mathrm{T}}\left(\boldsymbol{K}^{-1}x_1\right)}\sqrt{\left(\boldsymbol{K}^{-1}x_2\right)^{\mathrm{T}}\left(\boldsymbol{K}^{-1}x_2\right)}}\\&=\frac{x_1^{\mathrm{T}}\left(\boldsymbol{K}^{-\mathrm{T}}\boldsymbol{K}^{-1}\right)x_2}{\sqrt{\left(x_1^{\mathrm{T}}\left(\boldsymbol{K}^{-\mathrm{T}}\boldsymbol{K}^{-1}\right)x_1\right)\left(x_2^{\mathrm{T}}\left(\boldsymbol{K}^{-\mathrm{T}}\boldsymbol{K}^{-1}\right)x_2\right)}}\\&=\frac{x_1^{\mathrm{T}}\boldsymbol{\Omega}'_\infty x_2}{\sqrt{\left(x_1^{\mathrm{T}}\boldsymbol{\Omega}'_\infty x_1\right)\left(x_2^{\mathrm{T}}\boldsymbol{\Omega}'_\infty x_2\right)}}.\end{aligned} \tag{7}$$

2 Intrinsic parameter calibration based on stellar angular distance and the absolute conic (ICSAC)

The starlight passing through CCD optics focuses on the imaging targeted surface of the probe and forms a projection. The imaging model of the starlight could be depicted by central projection model, as shown in Figure 2, in which

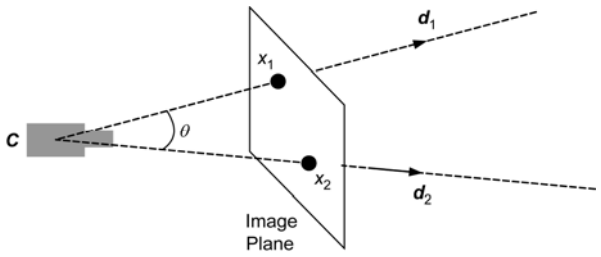

Figure 1 Ray included angle and absolute conic.

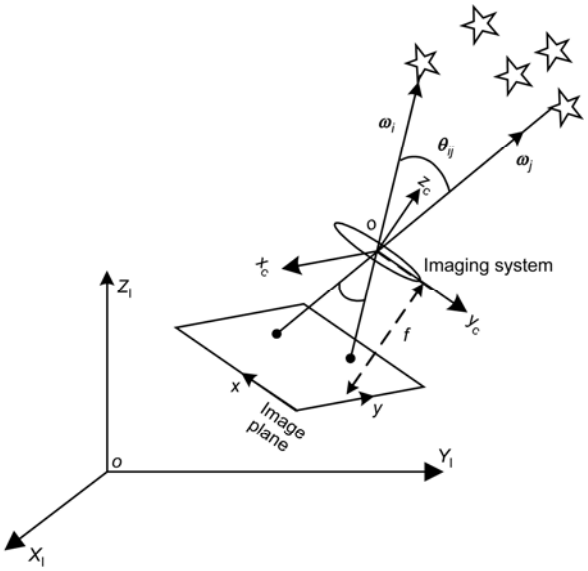

Figure 2 Pinhole imaging model.

O-$X_{\mathrm{I}}Y_{\mathrm{I}}Z_{\mathrm{I}}$ represents the inertial coordinate system, while o-$x_{\mathrm{c}}y_{\mathrm{c}}z_{\mathrm{c}}$ represents the camera coordinate system. Supposing the coordinate of the control point $\boldsymbol{P}_S$ is in the inertial coordinate system, the coordinate of camera coordinate system and the image coordinate system is (X, Y, Z), $(x_{\mathrm{c}}, y_{\mathrm{c}}, z_{\mathrm{c}})$, and (x, y) respectively.

The conversion relation between the inertial coordinate system and the camera coordinate system is

$$\begin{bmatrix}x_{\mathrm{c}}\\y_{\mathrm{c}}\\z_{\mathrm{c}}\end{bmatrix}=\boldsymbol{R}\begin{bmatrix}X\\Y\\Z\end{bmatrix}+\boldsymbol{T}, \tag{8}$$

where $\boldsymbol{R}$ represents 3×3 coordinate rotation matrix, namely, the gesture matrix of the camera, $\boldsymbol{T}$ represents the translation vector from the inertial coordinate system to the camera coordinate system.

The relation between the projected image coordinate of the control point $\boldsymbol{P}_S$ on the imaging surface and its coordinate in the camera coordinate system is

$$\begin{bmatrix}x\\y\\1\end{bmatrix}=\frac{1}{z_{\mathrm{c}}}\begin{bmatrix}f_x&0&x_0\\0&f_y&y_0\\0&0&1\end{bmatrix}\begin{bmatrix}x_{\mathrm{c}}\\y_{\mathrm{c}}\\z_{\mathrm{c}}\end{bmatrix}. \tag{9}$$

Substituting eq. (9) into eq. (8), it results in

$$\begin{bmatrix} x \\ y \\ 1 \end{bmatrix} = \frac{1}{z_c} \begin{bmatrix} f_x & 0 & x_0 \\ 0 & f_y & y_0 \\ 0 & 0 & 1 \end{bmatrix} \left(\boldsymbol{R} \begin{bmatrix} X \\ Y \\ Z \end{bmatrix} + \boldsymbol{T} \right). \tag{10}$$

The star, as the control point, is in infinite distance. During the conversion from the inertial coordinate system to the camera coordinate system, errors brought by the movement of an infinite point could be neglected, that is,

$$\begin{bmatrix} x_c \\ y_c \\ z_c \end{bmatrix} = \boldsymbol{R} \begin{bmatrix} X \\ Y \\ Z \end{bmatrix}. \tag{11}$$

Supposing $\boldsymbol{\omega}$ and $\boldsymbol{v}$ are the direction vectors of the star in the inertial coordinate system and the camera coordinate system, θ_{ij}^{I} represents the included angle between $\boldsymbol{\omega}_i$ and $\boldsymbol{\omega}_j$ rays in the inertial coordinate system, while θ_{ij}^{c} represents the included angle between $\boldsymbol{v}_i$ and $\boldsymbol{v}_j$ rays in the camera coordinate system, the relation between them is as follows:

$$\begin{aligned} \cos\theta_{ij}^{\mathrm{I}} &= \frac{\omega_i^{\mathrm{T}} \omega_j}{\|\omega_i\| \|\omega_j\|} = \frac{\left(\boldsymbol{R}^{-1} v_i\right)^{\mathrm{T}} \left(\boldsymbol{R}^{-1} v_j\right)}{\left\|\boldsymbol{R}^{-1} v_i\right\| \left\|\boldsymbol{R}^{-1} v_j\right\|} \\ &= \frac{v_i^{\mathrm{T}} v_j}{\|v_i\| \|v_j\|} = \cos\theta_{ij}^{\mathrm{c}}. \end{aligned} \tag{12}$$

The following conclusion concerning orthogonal transformation could be achieved: while choosing an infinite object as the observed target, the relation between the inertial coordinate system and camera coordinate system could be just approximately deemed as rigid rotation and the stellar angular distance is kept invariant.

According to the above conclusion, without considering the distortion and noise, a relation formula between the cosine of diagonal included angle θ_{ij}^{I} of any star and the absolute conic matrix and corresponding image points could be achieved:

$$\cos\theta_{ij}^{\mathrm{I}} = \frac{x_i^{\mathrm{T}} \boldsymbol{\Omega}'_{\infty} x_j}{\sqrt{\left(x_i^{\mathrm{T}} \boldsymbol{\Omega}'_{\infty} x_i\right)\left(x_j^{\mathrm{T}} \boldsymbol{\Omega}'_{\infty} x_j\right)}}. \tag{13}$$

As $\boldsymbol{\Omega}'_{\infty}$ represents symmetric matrix without loss of generality, supposing $\boldsymbol{\Omega}'_{\infty}$ is

$$\boldsymbol{\Omega}'_{\infty} = \begin{bmatrix} a & b & c \\ b & d & e \\ c & e & 1 \end{bmatrix}.$$

Recording $x_i = (\tilde{x}_i, \tilde{y}_i, 1)^{\mathrm{T}}$ and $x_j = (\tilde{x}_j, \tilde{y}_j, 1)^{\mathrm{T}}$ as the respective homogeneous coordinate of the projected image points of stars *i* and *j*, eq. (13) could be further settled as

$$F_{ij}(a,b,c,d,e) = x_i^{\mathrm{T}} \boldsymbol{\Omega}'_{\infty} x_j - \cos\theta_{ij}^{\mathrm{I}} \sqrt{\left(x_i^{\mathrm{T}} \boldsymbol{\Omega}'_{\infty} x_i\right)\left(x_j^{\mathrm{T}} \boldsymbol{\Omega}'_{\infty} x_j\right)}, \tag{14}$$

where

$$\begin{cases} x_i^{\mathrm{T}} \boldsymbol{\Omega}'_{\infty} x_j = a\tilde{x}_i\tilde{x}_j + d\tilde{y}_i\tilde{y}_j + 1 + b\left(\tilde{x}_j\tilde{y}_i + \tilde{x}_i\tilde{y}_j\right) \\ \qquad\qquad + c\left(\tilde{x}_j + \tilde{x}_i\right) + e\left(\tilde{y}_i + \tilde{y}_j\right), \\ x_i^{\mathrm{T}} \boldsymbol{\Omega}'_{\infty} x_i = a\tilde{x}_i^2 + d\tilde{y}_i^2 + 1 + 2b\tilde{x}_i\tilde{y}_i + 2c\tilde{x}_i + 2e\tilde{y}_i, \\ x_j^{\mathrm{T}} \boldsymbol{\Omega}'_{\infty} x_j = a\tilde{x}_j^2 + d\tilde{y}_j^2 + 1 + 2b\tilde{x}_j\tilde{y}_j + 2c\tilde{x}_j + 2e\tilde{y}_j. \end{cases} \tag{15}$$

Taking into account measurement noise, eq. (14) should be

$$\begin{aligned} & x_i^{\mathrm{T}} \Omega'_{\infty} x_j - \cos\theta_{ij}^{\mathrm{I}} \sqrt{\left(x_i^{\mathrm{T}} \Omega'_{\infty} x_i\right)\left(x_j^{\mathrm{T}} \Omega'_{\infty} x_j\right)} \\ &= F_{ij}(a,b,c,d,e) + n_e. \end{aligned} \tag{16}$$

Supposing the estimated value of $(a,\ b,\ c,\ d,\ e)^{\mathrm{T}}$ is $(\hat{a},\ \hat{b},\ \hat{c},\ \hat{d},\ \hat{e})^{\mathrm{T}}$, and $(\Delta a,\ \Delta b,\ \Delta c,\ \Delta d,\ \Delta e)^{\mathrm{T}}$ represents the parameter estimation error, eq. (17) can be achieved by conducting first order Taylor expansion at the estimated value in eq. (16):

$$\begin{aligned} \varepsilon_{ij} &= B_{ij} - F_{ij}(\hat{a},\hat{b},\hat{c},\hat{d},\hat{e}) \\ &= \begin{bmatrix} \dfrac{\partial F_{ij}}{\partial a} & \dfrac{\partial F_{ij}}{\partial b} & \dfrac{\partial F_{ij}}{\partial c} & \dfrac{\partial F_{ij}}{\partial d} & \dfrac{\partial F_{ij}}{\partial e} \end{bmatrix} \begin{bmatrix} \Delta a \\ \Delta b \\ \Delta c \\ \Delta d \\ \Delta e \end{bmatrix} + n_e \\ &= A_{ij} \begin{bmatrix} \Delta a & \Delta b & \Delta c & \Delta d & \Delta e \end{bmatrix}^{\mathrm{T}} + n_e, \end{aligned} \tag{17}$$

where the definitions of B_{ij} and A_{ij} are as follows:

$$\begin{cases} B_{ij} = x_i^{\mathrm{T}} \boldsymbol{\Omega}'_{\infty} x_j - \cos\theta_{ij}^{\mathrm{I}} \sqrt{\left(x_i^{\mathrm{T}} \boldsymbol{\Omega}'_{\infty} x_i\right)\left(x_j^{\mathrm{T}} \boldsymbol{\Omega}'_{\infty} x_j\right)}, \\ A_{ij} = \begin{bmatrix} \dfrac{\partial F_{ij}}{\partial a} & \dfrac{\partial F_{ij}}{\partial b} & \dfrac{\partial F_{ij}}{\partial c} & \dfrac{\partial F_{ij}}{\partial d} & \dfrac{\partial F_{ij}}{\partial e} \end{bmatrix}. \end{cases}$$

Supposing the number of effective stars projecting on the same field of view is $n \geqslant 4$, eq. (17) should be corrected as

$$\begin{aligned} \varepsilon &= A \begin{bmatrix} \Delta a & \Delta b & \Delta c & \Delta d & \Delta e \end{bmatrix}^{\mathrm{T}} + N_e \varepsilon_{ij} \\ &= B_{ij} - F_{ij}(\hat{a},\hat{b},\hat{c},\hat{d},\hat{e}), \end{aligned} \tag{18}$$

where N_e represents the error matrix brought by random noise, and

$$\begin{cases} A = \begin{bmatrix} \dfrac{\partial F_{12}}{\partial a} & \dfrac{\partial F_{12}}{\partial b} & \dfrac{\partial F_{12}}{\partial c} & \dfrac{\partial F_{12}}{\partial d} & \dfrac{\partial F_{12}}{\partial e} \\ \vdots & \vdots & \vdots & \vdots & \vdots \\ \dfrac{\partial F_{ij}}{\partial a} & \dfrac{\partial F_{ij}}{\partial b} & \dfrac{\partial F_{ij}}{\partial c} & \dfrac{\partial F_{ij}}{\partial d} & \dfrac{\partial F_{ij}}{\partial e} \\ \vdots & \vdots & \vdots & \vdots & \vdots \\ \dfrac{\partial F_{(n-1)n}}{\partial a} & \dfrac{\partial F_{(n-1)n}}{\partial b} & \dfrac{\partial F_{(n-1)n}}{\partial c} & \dfrac{\partial F_{(n-1)n}}{\partial d} & \dfrac{\partial F_{(n-1)n}}{\partial e} \end{bmatrix}, \\ \varepsilon = \begin{bmatrix} \varepsilon_{12} & \cdots & \varepsilon_{ij} & \cdots & \varepsilon_{(n-1)n} \end{bmatrix}^{\mathrm{T}}, \end{cases}$$

$(i = 1,\ 2,\ \cdots,\ i,\ \cdots,\ n-1;\ j = i+1,\ \cdots,\ n).$

Generally, the optimal solution $\hat{\boldsymbol{\Omega}}'_{\infty}$ of $\boldsymbol{\Omega}'_{\infty}$ in algebra sense could be achieved through finite iteration by least square iterative method.

Eq. (6) shows that $\boldsymbol{\Omega}^*_{\infty} = (\boldsymbol{\Omega}'_{\infty})^{-1}$ is the product of an upper triangular matrix and its transposition, and a real symmetric matrix can uniquely confirm such upper triangular matrix and its transposition ($\boldsymbol{\Omega}^*_{\infty} = \boldsymbol{K}\boldsymbol{K}^{\mathrm{T}}$) through Cholesky. Accordingly, the intrinsic parameter matrix $\boldsymbol{K}$ could be calculated.

The balancing optimization of the intrinsic parameters of the camera can be conducted through "bundle adjustment" method. As the projection of the star on the imaging surface is an echogenic mass with a radius of r, and its measurement error fulfills the Gaussian distribution, according to ref. [10], the maximum likelihood estimate of $\boldsymbol{K}$ in reprojection error sense could be achieved.

3 Static datum conversion

Vehicle-mounted theodolite platform is a typical unstable measurement platform, in which the most critical factor influencing the theodolite measuring result is the gesture variation quantity of vehicle-mounted platform relative to the geodetic coordinate system, namely, the absolute gesture variation quantity. According to the requirements of different tasks, the vehicle-mounted theodolite would be put into work outdoors, requiring quick and all weather operations of the correction system. However, the preparation of the vehicle-mounted theodolite platform at initial moment costs quite a long time, and is affected by outdoor environment, it is quite difficult for the leveling accuracy to fulfill the requirements. Therefore, we propose the correction method based on static datum conversion.

3.1 Cardinal principle

As shown in Figure 3, the gesture of static datum relative to the camera is expressed as conversion matrix $\boldsymbol{H}_{\mathrm{Bc}}$, that of the geodetic coordinate system relative to static datum coordinate system is expressed as conversion matrix $\boldsymbol{H}_{\mathrm{wB}}$, and that of the camera relative to the theodolite platform is expressed as conversion matrix $\boldsymbol{H}_{\mathrm{cu}}$. As the camera and the theodolite platform are fixedly linked, $\boldsymbol{H}_{\mathrm{cu}}$ would not vary with time.

Supposing the conversion matrices of static datum relative to the camera at initial moment and at t are $\boldsymbol{H}^0_{\mathrm{Bc}}$ and $\boldsymbol{H}^t_{\mathrm{Bc}}$ respectively, the coordinates of the control point $\boldsymbol{P}$ in the theodolite platform coordinate system at initial moment and at t are $\boldsymbol{P}^0_{\mathrm{u}}$ and $\boldsymbol{P}^t_{\mathrm{u}}$ respectively; the coordinates of $\boldsymbol{P}$ in the camera coordinate system at initial moment and at t are $\boldsymbol{P}^0_{\mathrm{c}}$ and $\boldsymbol{P}^t_{\mathrm{c}}$ respectively; the coordinate of $\boldsymbol{P}$ in the static datum coordinate system is $\boldsymbol{P}_{\mathrm{B}}$, the following relations exist:

$$\left.\begin{aligned} \boldsymbol{P}^0_{\mathrm{u}} &= \boldsymbol{H}_{\mathrm{cu}}\boldsymbol{P}^0_{\mathrm{c}}, \\ \boldsymbol{P}^t_{\mathrm{u}} &= \boldsymbol{H}_{\mathrm{cu}}\boldsymbol{P}^t_{\mathrm{c}}, \\ \boldsymbol{P}_{\mathrm{B}} &= (\boldsymbol{H}_{\mathrm{wB}}\boldsymbol{H}^t_{\mathrm{Bc}})^{-1}\boldsymbol{P}^t_{\mathrm{c}}, \\ \boldsymbol{P}_{\mathrm{B}} &= (\boldsymbol{H}_{\mathrm{wB}}\boldsymbol{H}^0_{\mathrm{Bc}})^{-1}\boldsymbol{P}^0_{\mathrm{c}}, \end{aligned}\right\} \Rightarrow \boldsymbol{P}^0_{\mathrm{u}} = \boldsymbol{H}_{\mathrm{u}_t\mathrm{u}_0}\boldsymbol{P}^t_{\mathrm{u}}, \tag{19}$$

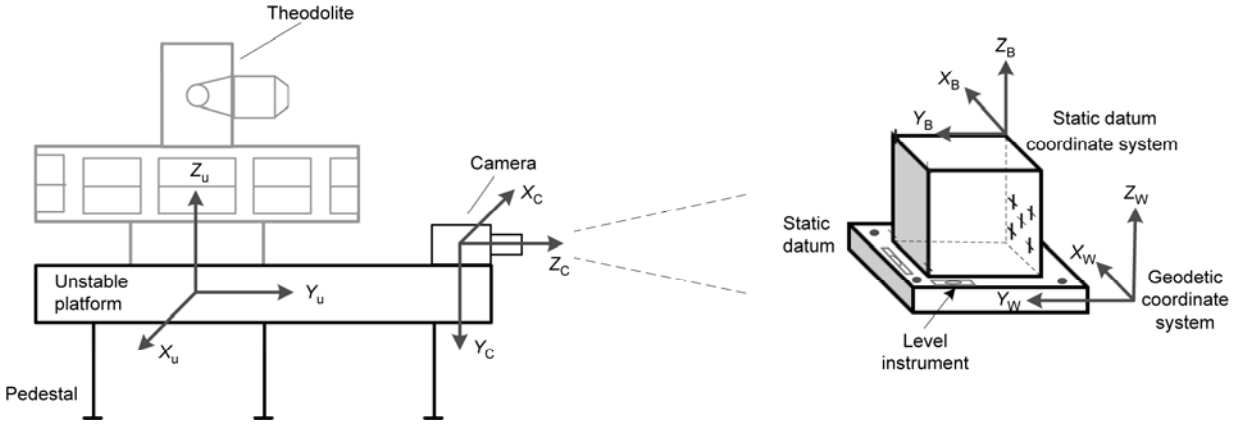

Figure 3 Schematic diagram of static datum conversion.

where

$$\boldsymbol{H}_{\mathrm{u}_t\mathrm{u}_0} = \boldsymbol{H}_{\mathrm{cu}}\boldsymbol{H}_{\mathrm{wB}}\boldsymbol{H}^{0}_{\mathrm{Bc}}(\boldsymbol{H}^{t}_{\mathrm{Bc}})^{-1}\left(\boldsymbol{H}_{\mathrm{wB}}\right)^{-1}\left(\boldsymbol{H}_{\mathrm{cu}}\right)^{-1}. \tag{20}$$

Partitioning of matrix $\boldsymbol{H}$ could achieve

$$\boldsymbol{H} = \begin{bmatrix} \boldsymbol{R}_{3\times3} & \boldsymbol{T}_{3\times1} \\ 0 & 1 \end{bmatrix}.$$

As translation vector has little impact on the result of theodolite measurement, we are just concerned with the gesture rotation relation between the theodolite platform coordinate system and the geodetic coordinate system at *t*. According to the multiplication principle of the partitioning matrix, eq. (20) could be expanded to

$$\begin{aligned}\boldsymbol{R}_{\mathrm{u}_t\mathrm{u}_0} &= \boldsymbol{R}_{\mathrm{cu}}\boldsymbol{R}_{\mathrm{wB}}\left[\boldsymbol{R}^{0}_{\mathrm{Bc}}\left(\boldsymbol{R}^{t}_{\mathrm{Bc}}\right)^{-1}\right]\boldsymbol{R}^{-1}_{\mathrm{wB}}\boldsymbol{R}^{-1}_{\mathrm{cu}} \\ &= \boldsymbol{R}_{\mathrm{cu}}\boldsymbol{R}_{\mathrm{wB}}\Delta\boldsymbol{R}_{\mathrm{c}}\boldsymbol{R}^{-1}_{\mathrm{wB}}\boldsymbol{R}^{-1}_{\mathrm{cu}}.\end{aligned} \tag{21}$$

The angular decomposition of this gesture matrix is the gesture shaking quantity (α, β, γ) of theodolite platform in the geodetic coordinate system at any moment. The correction of theodolite measured value could be completed based on the gesture shaking quantity [11].

3.2 Robust analysis

According to the form $\boldsymbol{R}_{\mathrm{u}_t\mathrm{u}_0} = \boldsymbol{R}(\Delta\boldsymbol{R})\boldsymbol{R}^{-1}$ in eq. (21), the following conclusion could be achieved: the installation error of the camera and theodolite platform and the partial calibration error of static datum are not added to the final gesture measurement result through linear superposition but reduce multiply. In this section, this is demonstrated mainly from two aspects such as mathematical derivation and simulation experiment.

3.2.1 Mathematical derivation

Without loss of generality, we just take into account the installation error of the camera and theodolite platform, and conduct a mathematical justification on the aforesaid conclusion. Defining $\tilde{\boldsymbol{R}}_{\mathrm{u}_t\mathrm{u}_0}$ and $\tilde{\boldsymbol{R}}_{\mathrm{u}_t\mathrm{u}_0}$ as the true value and measured value respectively of the gesture rotation matrix of the theodolite platform coordinate system at *t* and at initial moment, $\Delta\boldsymbol{R}_{\mathrm{cu}}$ is the installation error. $\tilde{\boldsymbol{R}}_{\mathrm{u}_t\mathrm{u}_0}$ and $\hat{\boldsymbol{R}}_{\mathrm{u}_t\mathrm{u}_0}$ could be expressed as

$$\begin{cases}\tilde{\boldsymbol{R}}_{\mathrm{u}_t\mathrm{u}_0} = \boldsymbol{R}_{\mathrm{cu}}\Delta\boldsymbol{R}_{\mathrm{cu}}\Delta\boldsymbol{R}_{\mathrm{c}}\Delta\boldsymbol{R}^{-1}_{\mathrm{cu}}\boldsymbol{R}^{-1}_{\mathrm{cu}}, \\ \hat{\boldsymbol{R}} = \boldsymbol{R}_{\mathrm{cu}}\Delta\boldsymbol{R}_{\mathrm{c}}\boldsymbol{R}^{-1}_{\mathrm{cu}}.\end{cases} \tag{22}$$

The error of the true value and the measured value is defined as

$$\begin{aligned}Error(\Delta\boldsymbol{R}_{\mathrm{cu}}) &= \left\|\tilde{\boldsymbol{R}}_{\mathrm{u}_t\mathrm{u}_0} - \tilde{\boldsymbol{R}}\right\|_F \\ &= \left\|\boldsymbol{R}_{\mathrm{cu}}\Delta\boldsymbol{R}_{\mathrm{cu}}\Delta\boldsymbol{R}_{\mathrm{c}}\Delta\boldsymbol{R}^{-1}_{\mathrm{cu}}\boldsymbol{R}^{-1}_{\mathrm{cu}} - \boldsymbol{R}_{\mathrm{cu}}\Delta\boldsymbol{R}_{\mathrm{c}}\boldsymbol{R}^{-1}_{\mathrm{cu}}\right\|_F \\ &= \left\|\boldsymbol{R}_{\mathrm{cu}}(\Delta\boldsymbol{R}_{\mathrm{cu}}\Delta\boldsymbol{R}_{\mathrm{c}}\Delta\boldsymbol{R}^{-1}_{\mathrm{cu}} - \Delta\boldsymbol{R}_{\mathrm{c}})\boldsymbol{R}^{-1}_{\mathrm{cu}}\right\|_F \\ &\leqslant \left\|\boldsymbol{R}_{\mathrm{cu}}\right\|_F\left\|\Delta\boldsymbol{R}_{\mathrm{cu}}\Delta\boldsymbol{R}_{\mathrm{c}}\Delta\boldsymbol{R}^{-1}_{\mathrm{cu}} - \Delta\boldsymbol{R}_{\mathrm{c}}\right\|_F\left\|\boldsymbol{R}_{\mathrm{cu}}\right\|_F \\ &\leqslant \lambda\left\|\Delta\boldsymbol{R}_{\mathrm{cu}}\Delta\boldsymbol{R}_{\mathrm{c}}\Delta\boldsymbol{R}^{-1}_{\mathrm{cu}} - \Delta\boldsymbol{R}_{\mathrm{c}}\right\|_F.\end{aligned} \tag{23}$$

From eq. (23), when the shaking quantity of the camera $\Delta\boldsymbol{R}_{\mathrm{c}} \to \boldsymbol{I}$, the $Error(\Delta\boldsymbol{R}_{\mathrm{cu}}) \to 0$. Under the extreme condition of $\Delta\boldsymbol{R}_{\mathrm{c}} = \boldsymbol{I}$, namely, the gesture of the camera remains unvaried, the installation error would not have any impact on the final measurement result. Under practical working conditions, the three-axis gesture shaking quantity of the theodolite platform (or the camera) is generally less than 30″ and the static datum conversion technique can weaken the gesture measurement error caused by installation error. This characteristic is of great significance in project realization, which can achieve higher measurement accuracy under equal hardware conditions and also reduce the hardware cost greatly under the same measurement accuracy.

3.2.2 Simulation verification

In the experiment of Monte Carlo, the static datum is 5 m away from the optic center of the camera with an imaging surface size of 1024×1024 pixels, the static datum is composed of 9 cooperative marks distributed within a square space of 0.5 m×0.5 m×0.5 m andthe extracted point extraction error distribution fulfills the Gaussian noise with condition of 0 mean value and 0.1 standard deviation. The measured value should be the azimuth and the pitch elevation angle of target to be measured and is the corrected measured value through the method proposed herein, not considering the camera calibration error. The result of the experiment is shown in Figure 4, Figures 4(a)−4(c) indicate that when the shaking range of the measurement platform is 0−30′, the correction accuracy of the azimuth and pitch angle would be higher than 10″, while Figure 4(d) indicates that the triaxial installation error is within 3°, the impact on the accuracy of the corrected correction result would be just 8″.

4 Correction method

The expression of *P* under two coordinate systems could easily be achieved from the spatial geometrical relationship in Figure 5:

$$\begin{cases}X_{\mathrm{W}} = D\cos E\cos A, \\ Y_{\mathrm{W}} = D\sin E, \\ Z_{\mathrm{W}} = D\cos E\sin A,\end{cases} \tag{24}$$

and

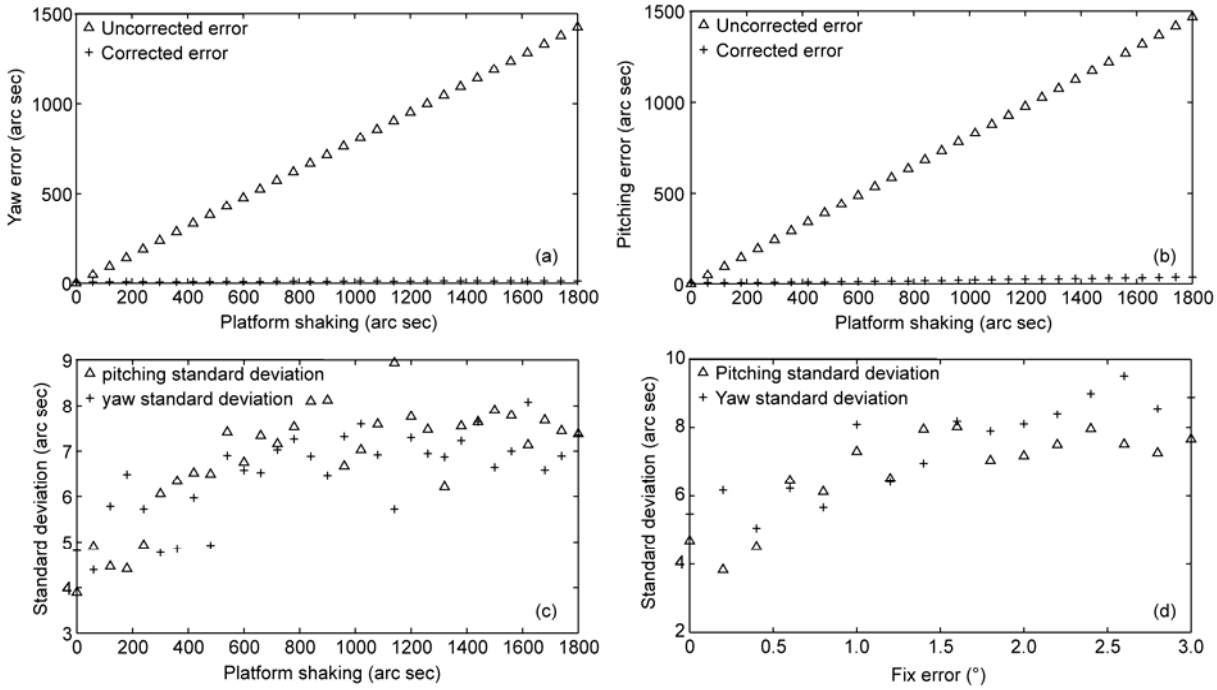

Figure 4 Result of the experiment of Monte Carlo.

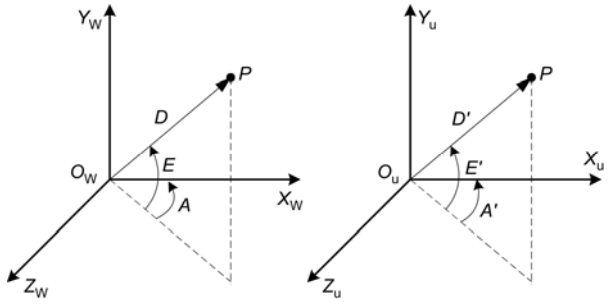

Figure 5 Geometrical relationship of the target in two coordinate systems.

$$\begin{cases} X_{\mathrm{u}} = D'\cos E'\cos A', \\ Y_{\mathrm{u}} = D'\sin E', \\ Z_{\mathrm{u}} = D'\cos E'\sin A'. \end{cases} \tag{25}$$

As the coincidence of the geodetic coordinate system and the theodolite platform coordinate system at initial moment, there would be

$$\begin{bmatrix} X_{\mathrm{W}} \\ Y_{\mathrm{W}} \\ Z_{\mathrm{W}} \end{bmatrix} = \boldsymbol{R}_{\mathrm{u}_t\mathrm{u}_0} \begin{bmatrix} X_{\mathrm{u}} \\ Y_{\mathrm{u}} \\ Z_{\mathrm{u}} \end{bmatrix} + \boldsymbol{T}_{\mathrm{u}_t\mathrm{u}_0}, \tag{26}$$

where $\boldsymbol{R}_{\mathrm{u}_t\mathrm{u}_0}$ represents the rotation matrix of the platform coordinate system transforming from t to the initial moment.

Substituting eqs. (24) and (25) into eq. (26), it results in

$$D\begin{bmatrix} \cos E\cos A \\ \sin E \\ \cos E\sin A \end{bmatrix} = D'\boldsymbol{R}_{\mathrm{u}_t\mathrm{u}_0}\begin{bmatrix} \cos E'\cos A' \\ \sin E' \\ \cos E'\sin A' \end{bmatrix} + \boldsymbol{T}_{\mathrm{u}_t\mathrm{u}_0}. \tag{27}$$

Dividing D on both sides of eq. (27) at the same time, it results in

$$\begin{bmatrix} \cos E\cos A \\ \sin E \\ \cos E\sin A \end{bmatrix} = \frac{D'}{D}\boldsymbol{R}_{\mathrm{u}_t\mathrm{u}_0}\begin{bmatrix} \cos E'\cos A' \\ \sin E' \\ \cos E'\sin A' \end{bmatrix} + \frac{1}{D}\boldsymbol{T}_{\mathrm{u}_t\mathrm{u}_0}, \tag{28}$$

where D and D' are the object distance, namely, the distance between the measured object and the theodolite, which is at least several thousands of meters. In the shaking quantity of the vehicle-mounted theodolite platform, the translation quantity is generally millimeter magnitude, translation $\boldsymbol{T}_{\mathrm{u}_t\mathrm{u}_0} \ll D$. Therefore, it could be approximately deemed that:

$$\frac{1}{D}\boldsymbol{T}_{\mathrm{u}_t\mathrm{u}_0} \approx 0, \quad \frac{D'}{D} \approx 1. \tag{29}$$

Substituting eq. (29) into eq. (28), there would be

$$\begin{bmatrix} \cos E\cos A \\ \sin E \\ \cos E\sin A \end{bmatrix} = \boldsymbol{R}_{\mathrm{u}_t\mathrm{u}_0}\begin{bmatrix} \cos E'\cos A' \\ \sin E' \\ \cos E'\sin A' \end{bmatrix}. \tag{30}$$

Substituting all the elements of $\boldsymbol{R}_{\mathrm{u}_t\mathrm{u}_0}$ into eq. (30) yields

$$\begin{cases} \tan A = \dfrac{r_{31}\cos E'\cos A' + r_{32}\sin E' + r_{33}\cos E'\sin A'}{r_{11}\cos E'\cos A' + r_{12}\sin E' + r_{13}\cos E'\sin A'}, \\ \sin E = r_{21}\cos E'\cos A' + r_{22}\sin E' + r_{23}\cos E'\sin A', \end{cases} \tag{31}$$

Where r_{11}–r_{33} are the corresponding elements of matrix $\boldsymbol{R}_{u,u_0}$.

A computational formula of the algebra correction method is given in eq. (31). Correcting the measured value of the measured target through the measured rotation matrix of the platform coordinate system relative to the geodetic coordinate system at any time the corrected pitch angle and azimuth [12] are achieved.

5 Experiments

5.1 Calibration experiment

A CCD camera was chosen with a pixel resolution of 1024× 1024 pixels design focal distance of 52 mm, pixel size of 3.45 μm×3.45 μm, and field of view of 20.5°. Under favorable weather conditions, the starry sky was observed at night and 100 pictures of the star were collected. After obtaining the statistics of the star map, complete the identification and extraction [13] of the star map through grid method [14] and Kalman filtering method based on the Singer model. A star map is given in Figure 6, the circle in the map is the position of the star identified through grid method. The coordinate position of the star in Figure 6 is given in Table 1. Due to the atmospheric refraction, the observed position of the star is different from the real position of the star. The observed height of the star minus the astronomical refraction equals the authentic height of the star. The larger the zenith distance of the star, the larger the astronomical refraction, but with the variation of temperature and atmospheric pressure, the astronomical refraction would be different. The theoretical elevation angle of the star would be achieved generally through the correction method of astronomical refraction in astronomical almanac [4, 15, 16].

After obtaining the accurate stellar angular distance, the intrinsic parameter of the camera was calibrated through the method based on the stellar angular distance and the absolute conic. Meanwhile, in order to further improve the accuracy of calibration, during the calculation of intrinsic parameter, the result was optimized through "bundle adjustment" and the result is shown in Table 2 in which the results of calibration obtained from ICSAC method and two-step method [17] (using 11cooperative mark points from different surfaces) and the root mean square error (RMS) value are listed. Where, the RMS value of ICSAC is the RMS value measured by pixels transformed from the RMS value measured by radian according to the ratio of the angular travel error (the absolute value of the difference between the stellar angular distance calculated by using the calibration parameter and the stellar angular distance in the ephemeris). While the RMS value of the two-step method is a little bit larger than that of ICSAC, for there is coupling between the intrinsic and external parameters during the process of the two-step method and the estimated error of gesture and displacement would count in intrinsic parameter estimation.

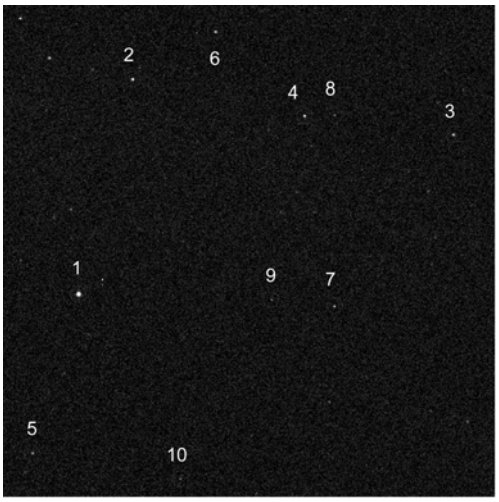

Figure 6 Star map and the identified result.

Table 1 The identified result of the star map

No.	Coordinates position of the star (pixels)	
	x	*y*
1	79.19565	301.7416
2	135.7851	77.96691
3	469.5401	135.0509
4	314.5726	115.6011
5	31.42671	467.1654
6	221.9541	28.40661
7	345.5889	314.4315
8	345.8454	114.7738
9	280.1721	307.6164
10	185.5078	493.9099

5.2 Experiment of static datum conversion method

As the theodolite could not get the true value of the azimuth and elevation angle of the measured target due to theodolite platform shaking, the verification of accuracy could not be achieved. However, the correction accuracy is mainly influenced by the gesture shaking quantity (rotation matrix) of the theodolite platform coordinate system relative to the

Table 2 Result of calibration experiment

Intrinsic parameter	ICSAC	Two-step calibration method
x_0 (pixels)	492.93	413.77
y_0 (pixels)	509.26	532.61
f (mm)	51.6582	50.6559
RMS (pixels)	0.04	0.1239

geodetic coordinate system at any time, and from eq. (31), it can be proved that the measurement accuracy and correction accuracy of gesture shaking quantity of the theodolite platform are at the same magnitude. Therefore, in this section, the measurement error of the three-axis gesture shaking angle is used as evaluation criteria and the specific experiment scheme is shown in Figure 7. The total station simulates the theodolite platform under practical conditions, with the camera and the eyepiece lens barrel fixed together and the transformational relation known, cooperative marks (9 infrared marker lights) fixed on the ground as the static datum; the distance between the total station and static datum is 15 m.

Taking the average value of the rotation matrix calculated from the first 10 images as the measured value [9] of the initial state of the total station, the variation of the three-axis gesture angle of the total station at any time relative to the initial state was calculated and the measurement error was defined as the difference between the measured value of the system and the measured data of the total station.

The choice of camera exposure time would have great impact on the measurement result. Therefore, under the condition of clear imaging, the shorter the camera exposure time, the higher the measurement accuracy. A research indicates that under normal working conditions, multi-level resonance could take place within the vehicle-mounted theodolite platform, but the high frequency 8–10 Hz component vibration is the strongest, that is, master vibration modal. Therefore, the requirement of the experiment would be fulfilled by setting the camera exposure time as 50 ms in the experiment.

The three-axis gesture variation of the camera measured in different rotation positions in the experiment is given in Figure 8(a). ΔAx, ΔAy and ΔAz represent pitching, yaw and rotation respectively. While the real time measurement error of different stably measured positions is given in Figure 8(b). According to the statistics, the standard error of errors in the figure is 1.9″, 1.5″, 1.7″.

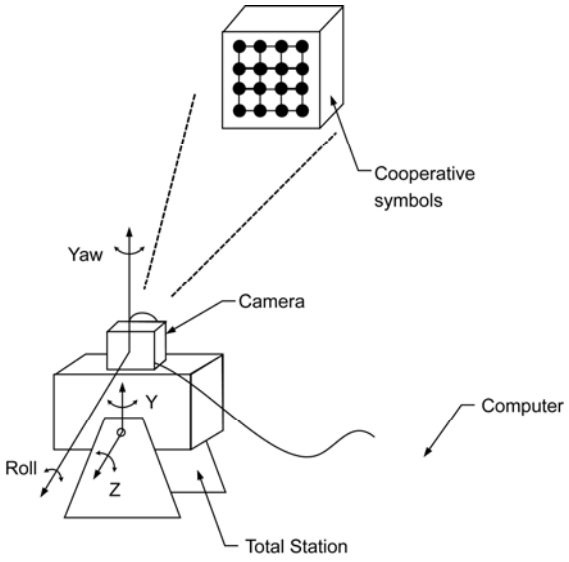

Figure 7 Schematic diagram of the experiment of static datum conversion method.

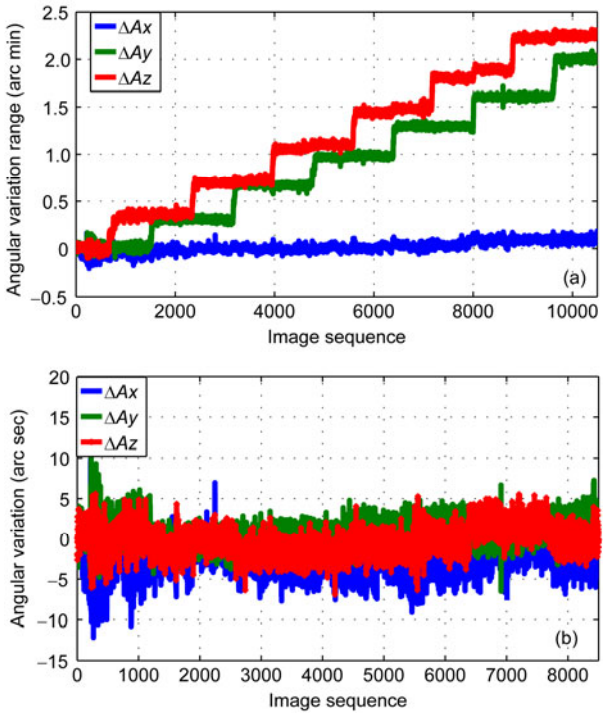

Figure 8 Data presentation of the measurement result of the experiment.

6 Conclusions

A correction method of non-landing measuring of the theodolite based on static datum conversion is proposed in this paper, mainly related to two key techniques, the intrinsic calibration and the static datum conversion. The independent intrinsic parameter calibration method based on the stellar angular distance and absolute conic could achieve decoupling calibration of intrinsic and external parameters and increase the accuracy of intrinsic parameter calibration. As to the issue that the preparation work of the theodolite before practical outdoor measurement tasks cost time and could hardly fulfill the accuracy requirement, a correction method based on static datum conversion is proposed in this paper, which could achieve higher measurement accuracy under the same hardware condition and reduce hardware cost enormously under the same requirement of measurement accuracy. According to the research in the paper, the following main conclusions could be achieved.

1) From the comparison of the results in Table 2, the accuracy of the camera intrinsic parameter calibration method based on stellar angular distance has been improved apparently compared with that of two-step method. The primary cause of this is that the method in the paper would not be

impacted by the evaluation error of external parameter, but in the two-step method, the evaluation error of the external parameter would result in the increase of the intrinsic parameter calibration due to the coupling of intrinsic and external parameters.

2) The theoretical derivation and simulation verification in Section 3.2 prove that the correction method of non-landing measurement of the vehicle-mounted theodolite based on static datum conversion could allow certain camera installation error. When the shaking range of the theodolite platform is below 30 min of arc, this method could weaken the gesture measurement error caused by installation to a large extent mainly because when $\Delta \boldsymbol{R}_{\mathrm{cu}} \to \boldsymbol{I}$, $\Delta \boldsymbol{R}_{\mathrm{cu}} \Delta \boldsymbol{R}_{\mathrm{c}} \Delta \boldsymbol{R}_{\mathrm{cu}}^{-1} \approx \Delta \boldsymbol{R}_{\mathrm{c}} \Delta \boldsymbol{R}_{\mathrm{cu}} \Delta \boldsymbol{R}_{\mathrm{cu}}^{-1}$, thus eliminating the impact of installation error.

3) The static datum conversion experiment indicates that under the condition of a 15-m distance between the camera and the static datum, the 3σ accuracy of the correction method of non-landing measurement of the vehicle- mounted theodolite proposed in the paper would exceed 10 s of arc. The error mainly comes from the intrinsic parameter calibration error of the camera, point extraction noise, CCD background noise, camera exposure time, etc. Moreover, the accuracy of this method is related to the proportion of the static datum on the imaging surface. The larger the proportion is, the higher the measurement accuracy will be. Ref. [8] gives out the concrete mathematical derivation.

However, while adopting the method in the paper, certain environmental requirement has to be fulfilled. If the temperature is too high or atmospheric disturbance is too severe, it could result in the deviation from the appropriate position of imaging points of static datum and the increase in point extraction error, the accuracy of final gesture calculating would be impacted. Therefore, the problem that needs focused research and resolution next is how to enhance the adaptive captivity of the method under severe environment.

The method proposed in the paper could be applied to and promoted in the field of shaking measurement of various unstable platforms and tiny structure transformation and, in principle, could also be used in solving the problem concerning observation area alignment caused by environment and temperature variation during earth observation from outer space.

This work was supported by the National Natural Science Foundation of China (Grant Nos. 11072263 and 11272347) and Program for New Century Talents in University.

1 Wang T, Tang J, Song L W. Correction of the measuring error of vehicular photoelectric theodolite (in Chinese). Infrared Laser Eng, 2012, 5(41): 1335–1338
2 Jiang W W, Gao Y G, Feng D Y, et al. Corrected error of base-plane for vehicle-borne photoelectric theodolite (in Chinese). Acta Astronaut, 2009, 30(12): 1638–1641
3 Li Z, Wu Z Y, Tong G, et al. Pointing error correction for vehicular platform theodolite (in Chinese). Opt Prec Eng, 2010, 18(4): 921–927
4 Zhang Y Y. The research of vehicle plane distortion measuring and error emendation technology (in Chinese). Doctoral Dissertation. Beijing: Graduate University of Chinese Academy of Sciences, 2003
5 Tong G, Wang F. Analysis and correction for influence of vehicle platform deformation on measuring errors (in Chinese). Opt Prec Eng, 19(4): 775–781
6 Zhang D M, Shang C M, Qiao Y F. The research of deformation measurement technology of vehicle flat in photoelectric theodolite (in Chinese). Laser Infrared, 2005, 35(6): 435–437
7 Yu Q F, Sun X Y, Jiang G W, et al. Relay camera videometrics based conversion method for unstable platform to static reference. Sci China Tech Sci, 2011, 54: 1017–1023
8 Shang Y, Yu Q F, Zhang X H, et al. Analytical method for camera calibration from a single image with four coplanar control lines. Appl Opt, 2004, 43(28): 5364–5368
9 Zhang X H, Zhang Z, Li Y, et al. Robust camera pose estimation from unknown or known line correspondences. Appl Opt, 2012, 51(7): 936–948
10 Hartley R, Andrew Z Multiple View Geometry in Computer Vision. Hefei: Anhui University Press, 2002
11 Zhang Z. Research on measurement error correction of vehicle photoelectric theodolite working on the quasi-moving base (in Chinese). Dissertation for Masteral Degree. Changsha: National University of Defense Technology, 2007
12 Zhou J. Study on optical measurement techniques based on unstable and moving platforms in shooting range (in Chinese). Doctoral Dissertation. Changsha: National University of Defense Technology, 2012
13 Singer R A. Estimating optimal tracking filter performance for manned manervering targets. IEEE T Aerosp Electr Syst, 1970, 6(4): 473–483
14 Rufino G, Accardo D. Enhancement of the centroiding algorithm for star tracker measure refinement. Acta Astronaut, 2003, 52(2): 135–147
15 Liu H B, Wang J Q, Tan J C, et al. Autonomous on-orbit calibration of a star tracter camera. Opti Eng, 2011, 50(2): 023604
16 Wang Z, Xiao P F, Gu X F, et al. Uncertainty analysis of cross-calibration for HJ-1 CCD camera. Sci China Tech Sci, 2013, 56: 713–723
17 Yu Q F, Shang Y. Videometrics: Principles and Researches. Beijing: Science Press, 2009